Spatial and Temporal Dynamics of Individual Step Merging Events on Ni(977) Measured by Scanning Tunneling Microscopy

T. P. Pearl[†] and S. J. Sibener*

The James Franck Institute and the Department of Chemistry, The University of Chicago, 5640 S. Ellis Avenue, Chicago, Illinois 60637

Received: March 28, 2001; In Final Form: April 26, 2001

Step dynamics induced by the chemisorption of oxygen on Ni(977) at low coverages and elevated temperatures have been studied using scanning tunneling microscopy (STM). Previous experiments using both local probe and scattering techniques have assessed the surface reconstruction behavior and structural transformations for this vicinal system. At temperatures above 390 K, the surface is capable of undergoing step doubling or merging if exposed to small amounts of oxygen. These double steps exist up to 565 K, where step-adsorbed oxygen dissolves into the nickel lattice destabilizing this morphology. Real-time STM measurements have been made on the behavior of individual merging events as a function of local step density, and hence local oxygen concentration at step edges, at 465 K. Results indicate that there is an optimal oxygen coverage, corresponding to complete titration of the single step density, that enables fast step merging to occur. An areal sweep rate of $\sim$60 Å^2 s^{-1} was found for step doubling under these conditions. For oxygen coverages greater than the single step density in which four adjacent single steps are embedded in an otherwise doubled local environment, step merge motion was punctuated in time. We attribute this observation to local energetics, in which specific structural fluctuations, including adsorbate step decoration and local step and kink configurations, enable the doubling transition. Moreover, under these same conditions, strong spatial and temporal correlations were observed for the coalescence of adjacent pairs of steps. These time-lapse STM studies advance our understanding of the atomic-level mechanisms which contribute to the initial stages of oxidation and facetting for metallic surfaces.

Introduction

There is great interest in determining how defects, including deviations from perfect crystalline planes, influence surface reaction mechanisms, rates, and equilibrium morphology. Numerous examples of surface reactions studied on a local scale have been shown to exhibit anisotropic behavior where different reaction rates and products are observed as a function of surface features or defects.[1−5] The presence of disruptions in surface geometry is capable of introducing surface structural instabilities as well as creating inhomogeneous substrate−adsorbate interactions. One way of quantifying the impact of a particular type of defect, such as a monatomic step, on surface phenomena is to employ an intentionally stepped surface geometry. Careful preparation of stepped or vicinal surfaces yields a reproducible, narrow terrace width distribution with long-range coherence for the step edges. These systems can be examined using both reciprocal-space and real-space local probe techniques to assess the degree to which the ensemble of steps is influencing a surface process with respect to surface averaged or nanoscale properties. Both experimental and theoretical studies have focused on the differences introduced by steps as compared to the flat surface counterpart (the surface from which the vicinal was derived) with respect to the behavior of the clean surface and interfacial structures.[6−8]

An issue of interest in many vicinal surfaces is the structural transitions driven by thermal or chemical forces. Stepped metal surfaces in particular have been observed to undergo adsorbate driven surface reconstructions with respect to step heights and terrace widths.[9] The delicate thermodynamic balance directed at minimizing surface free energy determines the equilibrium crystal shape, and high index surfaces are particularly prone to shifts in their surface free energy minima.[10] The entropy of step wandering and the orientation of step edge dipoles, both of which contribute to the step-step interaction behavior, are susceptible to modification with the introduction of strongly interacting adspecies.[11] Various studies on the oxygen-driven reconstruction behavior of Ni(977) have been performed using helium scattering, electron diffraction, and, most recently, STM.[12−14] The combination of STM and reciprocal-space scattering techniques has been employed to uncover mechanistic details for the structural phase transitions, such as rate-limiting processes and the sensitivity of the surface reconstruction to oxygen exposure.

To further expand our understanding of the propensity of local morphology to adapt different equilibrium configurations, we have chosen to analyze the behavior of individual step merges that occur for oxygen-mediated step coalescence on Ni(977). This stepped metal surface is a 7.01° miscut of the (111) plane in the [2$\bar{1}\bar{1}$] direction, resulting in (111) terraces 8 atomic rows wide, separated by monatomic (100) steps (Figure 1). When exposed to oxygen at elevated temperatures, 390−565 K, the single-step arrangement shown in Figure 1 evolves into the doubled structure where the terraces become 15 atomic rows wide and the risers are twice as high. The lower end of the reconstructive range is bounded by step edge mobility, while

* Corresponding author. E-mail: s-sibener@uchicago.edu.
[†] Present address: Department of Chemistry, The Pennsylvania State University, 152 Davey Laboratory, University Park, PA 16802.

10.1021/jp011165c CCC: $20.00
Published on Web 06/14/2001

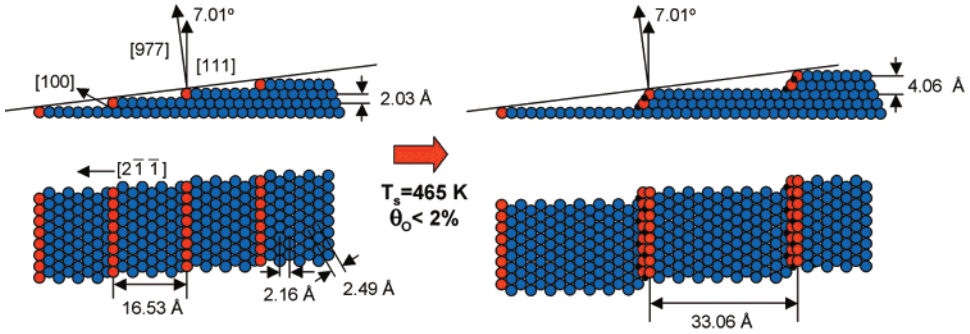

Figure 1. Schematic illustration of the step configurations for Ni(977). Several crystallographic dimensions and high-symmetry directions are indicated. The clean, single-step structure for this surface is composed of (111) terraces 8 atomic rows wide, separated by monatomic (100) risers. In the presence of small amounts of oxygen at elevated temperatures, this surface undergoes a step doubling transition. For the doubled surface, the (111) terraces extend to 15 atomic rows, and the height is doubled.

the temperature for dissolution of step edge-adsorbed oxygen limits the upper end. We report on the nature of individual coalescence events, i.e., two single steps merging into a double step, and how the speed at which such a merge occurs is influenced by local oxygen concentration at the step edges.

Many STM studies have been performed on stepped surfaces along with accompanying theoretical modeling using STM data, but very few initiatives have been aimed at resolving the local dynamics of how steps coalesce. Surface mass transport processes necessary to achieve multiple structural phases have not been investigated extensively in real-time on a microscopic scale. High-temperature STM work by Sudoh et al. on facet growth kinetics on vicinal Si(113) has been reported recently.[15,16] Song et al. also studied the kinetics and facetting of this complex system using X-ray scattering and AFM.[17] Vicinal semiconducting systems, however, undergo more severe facetting or step bunching for the clean system compared to stepped metals. While the step bunching process on silicon is reminiscent of the step doubling in our system, the class of reconstruction is remarkably different. The nascent structure for the Ni(977) is stable with respect to thermally driven facetting, and its surface reconstruction is a chemically triggered event. Oxygen at low concentrations mediates step merging events at elevated temperatures to produce a step arrangement that is unstable when further exposed to oxygen and at temperatures above which oxygen dissolves into the bulk. The fact that this surface reconstruction is mediated by the introduction of an adsorbate in addition to the relatively long time scale over which the entire process occurs makes this system particularly tractable for elevated-temperature STM imaging.

By using real-time imaging of the step doubling that occurs, we have been able to extract step merging speeds. The events that we monitored were triggered by the exposure of oxygen so STM measurements of merging events could be performed at early stages. In a related study, we reported detailed observations from STM data on the step doubling process.[13,14] Step coalescence was found to proceed by zippering of steps as opposed to adatom migration across a terrace from one step to an adjacent one. Merging of steps is initiated by a point contact or localized bulging of one step toward its downstairs neighbor, and coalescence proceeds in both step edge directions after this contact is made (Figure 2). The step edge for the newly formed double step is located at the downstairs step. Similar behavior was observed on the vicinal Si(113) surface mentioned above.[15−17] Adjacent step bunches were observed to zip together as a result of a short-range attractive step−step interaction. On the basis of the $^1/_6$ power law variation over time of the terrace size during facetting, the rate-limiting step for bunching of steps was designated as the time for collisions of adjacent steps due

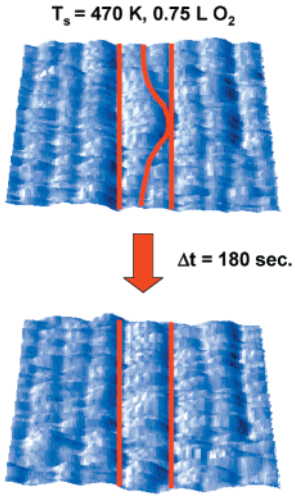

Figure 2. An individual step merging event resolved in time where the two images illustrate the initial point contact followed by zippering in both directions along the step edge. 350 Å × 350 Å image area shown with T_{xtal} = 470 K and 0.75 L O_2 exposure.

to their entropic meandering. Because of the nature of STM data acquisition at elevated temperatures, however, measurements on Si(113) facetting of the clean surface were limited to imaging at later stages in the process, consequently missing the commencement of an individual merging event. Using the oxygen triggering mechanism on Ni(977), we were able to observe the contact necessary between steps for a merge to proceed. These observations confirm theoretical predictions made by Khare et al. using Monte Carlo simulations on step doubling reconstructions.[18]

Experimental Details

Experiments were performed in a UHV chamber with a base pressure of 5.5×10^{-11} Torr that houses an STM for elevated temperature imaging and is equipped with standard sample cleaning and characterization tools. Procedural details for elevated temperature imaging and the design of the proximity heater are outlined elsewhere.[19] The microscope used in the system is an Omicron MicroSTM supported by a Viton elastomer stack attached to a flange. A proximity heater positioned directly behind the sample in the STM was used to produce elevated temperatures. Mechanically cut 90% Pt/10% Ir tips were used for all experiments. Images were recorded in constant current mode with a tunneling current of 1 nA and a 100 mV positive bias applied to the sample. While these tunneling conditions place the tip relatively close to the surface and thereby introduce the possibility of tip-induced processes,

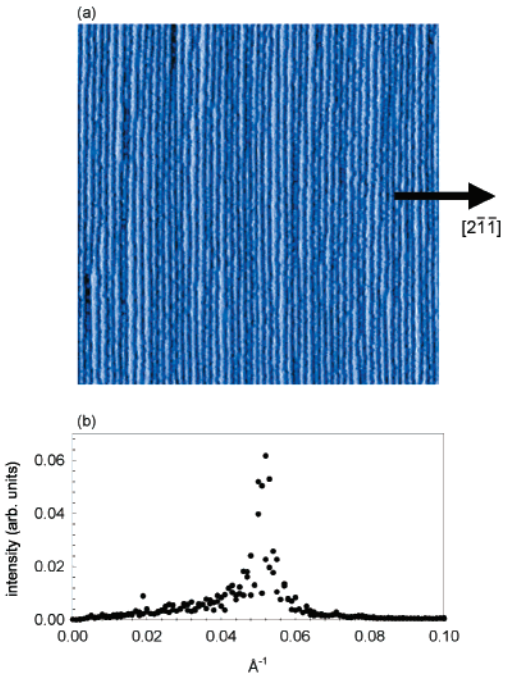

Figure 3. (a) STM image (1000 Å × 1000 Å area) of Ni(977) at 465 K taken with 100 mV positive sample bias and 1 nA tunneling current. A well-prepared surface will exhibit step width coherence for single steps over hundreds of angstroms. The downstairs direction for the step train is indicated. (b) Fourier transform of the clean surface indicates the high degree of ordering in the imaged region.

no preferential step motion along the scan direction was observed at the elevated temperatures studied. Scanning the surface at lower temperatures, outside of the range for doubling to occur on the surface, also revealed no effect of the tip on the mobility of the steps. Real-time STM sequences were recorded at 465 K. This particular temperature was chosen to ensure that step mobility would not be rate-limiting in the process of step merging. The goal of the experiment was to determine how step coalescence proceeds for different local oxygen concentrations at the step edges. Images were typically recorded in 20−40 s over a 1000 Å × 1000 Å range using a 300 × 300 pixel map. Time scales involved for this particular surface reconstruction enable the STM to resolve the dynamics.[12] Oxygen dosing was performed by chamber backfilling with high-purity O_2 using a high-precision leak valve located in proximity to the STM. Exposures listed reflect the approximate effective exposure (1/10 of that expected from the backfilling pressure alone) of a sample region illuminated by the STM tip. During time-lapse imaging at elevated temperature, drift compensation would be achieved by monitoring consecutive frames and manually correcting for systematic shifts in the image area.

An STM experiment would start by locating a well-ordered region of single steps at 465 K after a sputter and anneal cycle on a separate sample preparation stage. Figure 3 shows an array of single steps imaged at elevated temperature which can be characterized by a narrow terrace width distribution and sharp Fourier transform performed across the step edges. After a favorable region for an experiment was located, STM scanning would be paused, oxygen would be dosed, and imaging would be resumed once the oxygen exposure was complete (10−60 s). Successive images would be recorded for typically 1 h or until structural evolution in the region had reached an asymptotic limit. Once an entire sequence was collected, consecutive images would be compared to track changes that occurred. If a coalescence event took place, then we would monitor its behavior frame-by-frame, being careful not to associate any drift in imaged area with a physical change in step merge length. Since we were monitoring one area continuously as opposed following pairs steps with the STM as they merged on the surface, events that occurred within the region as well as those that started elsewhere and zipped their way into the field of view were monitored. Merge length was tracked by following the leading edges of the coalescing pair, as shown in Figure 4. Often, only one leading edge of a merging event could be tracked even though once paired, zippering proceeded in both directions. Various internal references could be used to measure step lengths. Any variation in imaged area from one image to the next was determined by observing the motion of multiple pinned step features that remained stationary throughout the imaging sequence. Relative motions of step merges would also act as landmarks to determine the real step motion, as opposed to drift effects. Regions of varying step density, from exclusively singled to a strong mix of single and double steps, would be exposed to oxygen to determine how the overall rate of doubling and the coalescence velocity were affected by the local oxygen concentration at step edges.

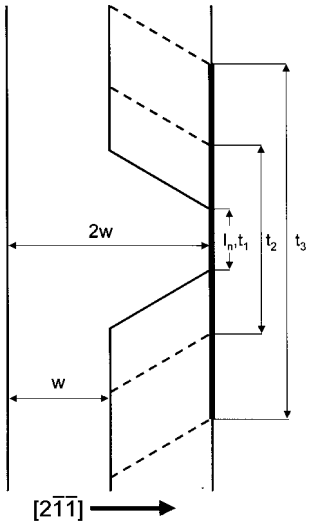

Figure 4. Illustration of measured parameters used to determine step merging speeds for a pair of coalescing steps.

Results and Discussion

Step merging speeds were calculated where the length of coalescence for a pair of steps was plotted as a function of time. An example of a single coalescence event being resolved by STM in real-time after an effective exposure of 0.15 L O_2 is shown in Figure 5. The sequence shows two steps merging as a function of time, where the merged step length increases at a steady rate, as shown in the plot in Figure 5. The length of this step merge and other selected events that occurred in the rest of the region from which Figure 5 splices were extracted are plotted versus time in Figure 6. The coalescence recorded is the total length of a merged pair and not just the distance in one step edge direction measured from the initial merge point. This particular region started with almost exclusively single steps and was dosed with an oxygen exposure that would correspond to step edge saturation. From linear fits to each of the events tracked in this particular area, step velocities in the range of 2.8−4.9 Å s^{-1} were extracted, yielding an average step merge speed of 3.7 Å s^{-1}. The average areal sweep rate for this set of merges, which is the step merge speed measured at the step

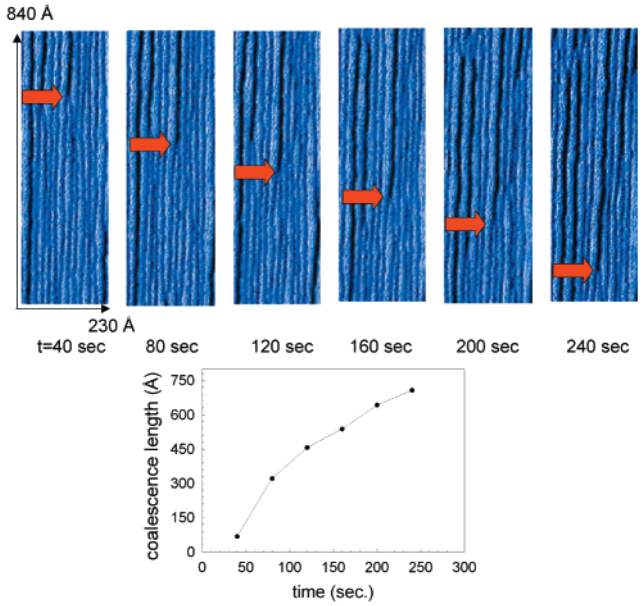

Figure 5. Sequence of images (840 Å × 230 Å) showing a step merging event for one pair of steps at 465 K after a dose of 0.15 L O_2. The arrows highlight the change in the length of the merged pair. The time between images is 40 s; imaging conditions used were 1 nA tunneling current and 100 mV positive sample bias.

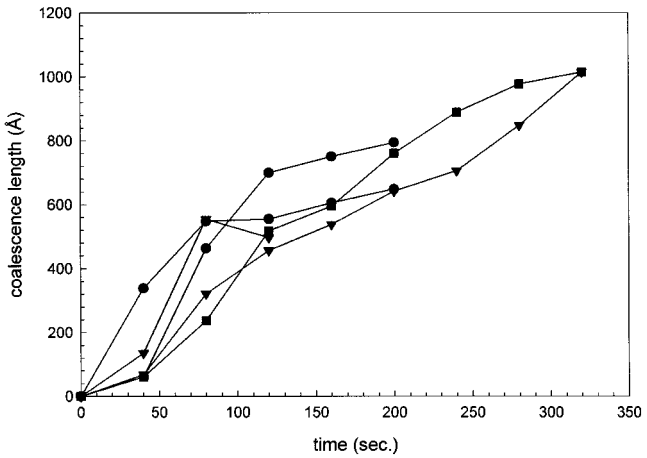

Figure 6. Coalescence length vs time for five merging events for 0.15 L O_2 exposure. The average merging speed is 3.7 Å s^{-1} using linear fits to the merge profiles. In plotting coalescence length vs time, t = 0 s corresponds to the time at which we were able to observe initiation of that particular event and not necessarily the time at which oxygen was dosed.

edge multiplied by the width of the propagating step (~16.5 Å), corresponds to ~60 $Å^2$ s^{-1}.

To test the sensitivity of the step doubling process to oxygen exposure, we started with a region of single steps and applied sequential doses. Figure 7 illustrates both the overall structural evolution of the surface and the coalescence for individual merging events monitored over time. The top panel represents the overall reconstruction occurring in the monitored area using the normalized intensity for both single and double-step fast-Fourier transform (FFT) peaks. A one-dimensional FFT of each image in the sequence was performed across the terraces in the downstairs direction; FFT peaks corresponding to single and double steps were integrated and normalized. Noted on the plot are the times when imaging would be paused and small sequential amounts of oxygen injected. The changes in surface reconstruction rate are a consequence of these applications of additional oxygen to the system. As the oxygen concentration

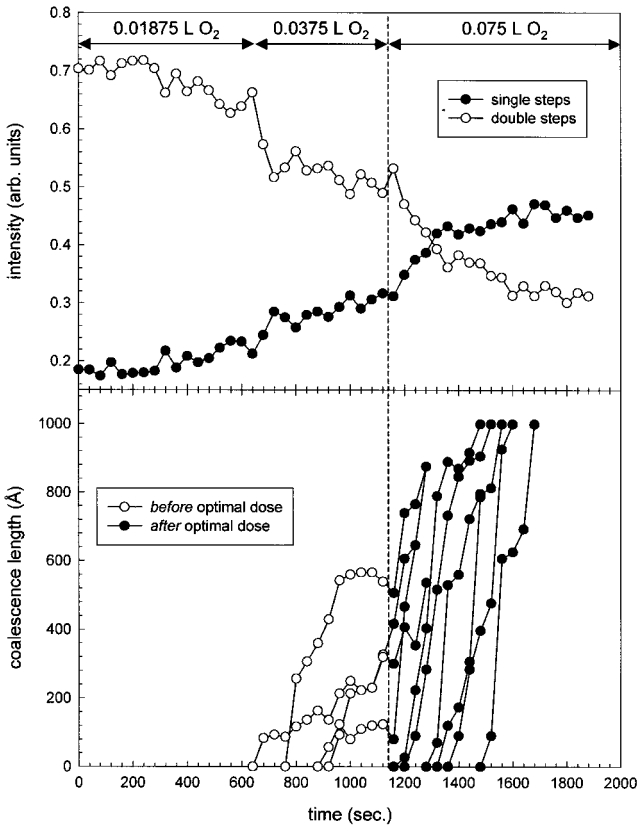

Figure 7. Demonstration of the sensitivity of step doubling to sequential doses of oxygen. The top panel shows the evolution of single- and double-step populations measured by FFT and the bottom panel shows the rapid increase in the number of merging events when the cumulative oxygen exposure reaches an optimal amount for step merging. The surface was initially given an effective dose of 0.01875 L O_2. After 600 s of monitoring the region, an additional dose of oxygen was supplied to give a cumulative exposure of 0.0375 L O_2 and finally at 1100 s, and the total exposure to the region was increased to 0.075 L O_2.

on the surface approaches step edge saturation, the density of merging events increases, as seen in the lower panel. The response of the system to a seemingly ideal oxygen concentration is dramatic where the rate of coalescence for an individual step merge is at its maximum for ~0.15 L cumulative oxygen exposure.

In other sequences, a region of steps containing both single and double steps was exposed to the same oxygen dose. A variety of different results appeared with respect to step merging speeds, indicating sensitivity to the initial local configuration of single and double steps. Two regions of differing step density before addition of oxygen are shown in Figure 8. Plotted beside each image are representative step merging events that occurred in each region after the addition of 0.15 L O_2. When the same exposure is given to both of these regions, we see a 5-fold difference in average step merge speed. There is also a broader distribution of speeds for the region of mixed single and double steps. An area that initially has more double steps before being exposed to oxygen will have a lower step density than an area that is composed exclusively of single steps. It is clear that the local concentration of oxygen on the step edges, which is determined by number of available step edge sites, strongly influences the rate at which single steps merge.

Another interesting regime is in the limit of high coverage where both the terraces and step edges are largely covered with oxygen. Figure 9 shows the time-resolved coalescence of two neighboring pairs of steps, i.e., four adjacent single steps,

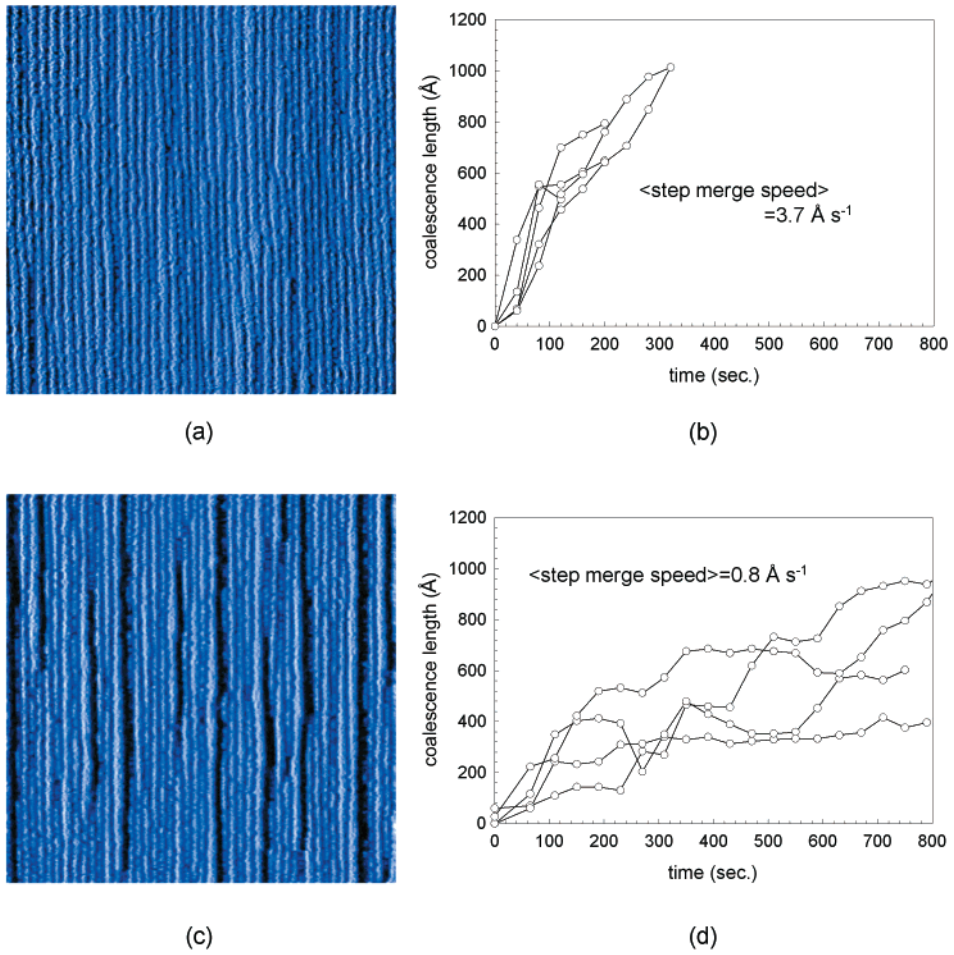

Figure 8. (a) A 840 Å × 840 Å region of well-ordered single steps before exposure to oxygen at 465 K. (b) A collection of different step merging events that occurred in region a after exposure to 0.15 L O_2. (c) A 840 Å × 840 Å region with a mix of single and double steps before exposure to oxygen. (d) A collection of merging events that occurred in panel c after exposure to 0.15 L O_2. The speed of step merging for individual events is faster for a region that starts with well-ordered single steps.

embedded in a local environment that is completely doubled. Punctuated jumps of zippering occur between long delays or gradual increases in merging. The zippering rate during these jumps is the same as that measured for merging steps that started in a more singled environment. This indicates that there is most likely an ideal concentration or configuration of oxygen atoms at the step edges that enable the steps to merge rapidly. *There is a remarkable correlation between the merge jumps of these two neighboring pairs of coalescing steps*. This inter-communication between adjacent merging events was not evident in the limit of solely step edge decoration with oxygen in a well-ordered region of single steps.[14]

The key feature in the analysis of individual merging events occurring at different relative oxygen coverages at the step edge is that the maximum coalescence speed for rapid zippering is the same regardless of exposure and step density. The results seem to indicate that the oxygen coverage in the regime where both the terraces and the step edges are largely decorated affects the rate of doubling. Both the local geometry of the steps, including kink configurations of the steps, and the local oxygen step decoration influence the rate of coalescence. The local concentration of oxygen at a given step edge will be affected by the ability of the oxygen to diffuse along the step edge and by the competing mechanism of dissolution into the terraces. A recent study of oxygen overlayers on this stepped surface suggests inhomogeneous dissolution, with pathways to incorporation of oxygen into the nickel lattice occurring at lower temperatures than on the flat Ni(111) counterpart.[20] It was not possible to atomically resolve the adsorbed oxygen atoms on the steps at 465 K that would have enabled us to confirm details regarding the role of oxygen and the true level of reconstruction sensitivity to oxygen aggregation at edges.

To quantify the energetics and kinetics involved in driving zippering of adjacent steps, we employ the model for step motion proposed by Sudoh et al. that includes a dissipation of line tension for merging step pairs and a short-range attractive interaction between steps.[16] Surface free energy, *f*, can be expressed as

$$f = f_o + (\beta_o - ST)\rho + g\rho^3 \qquad (1)$$

where the f_o is the free energy associated with the terrace, $\beta_o - ST$ is the free energy for step creation, g determines step-step interactions, and ρ is proportional to the step density.[21] When a step edge makes contact with a (100) step face, the local surface free energy will be determined by the competition between energy gained from the attractive interaction in forming the (100) microfacet in the f_o term and the energy lost from increasing the step edge length due the increase in entropy. Using the contact angle between steps that are merging, which implicitly corresponds to the local minimum in surface free energy, we are able to extract an attractive energy for the step−step interaction. Analysis and calculations yield an attractive energy, E_a, of ∼2.5 meV Å^{-1}.[13] This value corresponds to the

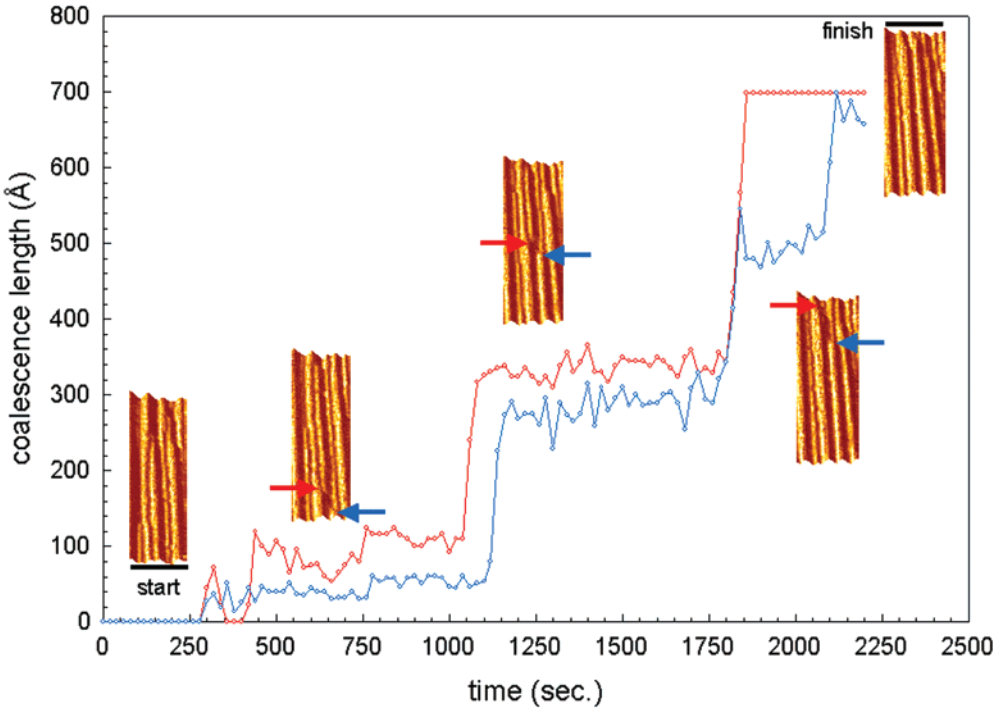

Figure 9. Example of merging behavior for two neighboring pairs of single steps embedded in a region of double steps for a dose of 0.15 L O_2. Plotted is the length of the two merged pairs as a function of time. Inserted in the figure are splices of images (750 Å × 100 Å) showing the two pairs of single steps. The images are placed at the points along the plot after a rapid merge event has occurred. Arrows indicate the position of the two step merges as they propagate. The punctuated jumps exhibited by both pairs have merging speeds equivalent to the average speed measured for a singled region with 0.15 L O_2 exposure. Note the remarkable correlation of motion of adjacent doubling events under these conditions.

difference in step formation energy costs for two single steps, as opposed to one double step. This relatively low attractive energy indicates that doubling is principally driven by the thermodynamically favorable formation of oxygen decorated (100) step faces.

Step zippering behavior can be modeled[16] as a stable step profile, $f(y)$, where the y direction is along the step edge, propagating with a constant velocity, υ

$$f(y) = L - L\exp\left(\frac{-y\tan\theta}{L}\right) \tag{2}$$

and

$$\upsilon = \Gamma_n\beta_n\frac{\tan\theta}{kTL} \tag{3}$$

where L is terrace width that is propagating during the merge. The areal rate of zippering, υL, is a constant that depends on the attractive interaction energy (dependent on contact angle, θ), step formation energy, β_n, and the mechanism for surface mass transport represented by the step mobility, Γ_n. By using a step formation energy, β_1, from a recent calculation by Vitos et al. on energy cost for monatomic steps on Ni [111]×[100] surfaces,[22] eqs 2 and 3 yield a step mobility of 82.5 $Å^3\ s^{-1}$. The time constants associated with both the collision of two steps and the subsequent zippering can be estimated using values for Γ_n and β_n. The time constants for zippering and collisions between steps can be described in terms of the collision distance for two adjacent steps, D[16]

$$\tau_{zip} = \frac{D}{\upsilon} = \frac{\beta L^2}{kT}\cdot\frac{1}{\upsilon} \tag{4}$$

$$\tau_{coll} \cong \frac{D^2kT}{\Gamma\beta} = \frac{\beta L^4}{\Gamma kT^*} \tag{5}$$

This ratio, however, of the time constants, $\tau_{coll}/\tau_{zip} = \upsilon L^2/\Gamma = 12$ shows that the time associated with collisions is longer than for that for zippering of the steps. This ratio however is much smaller than the factor of 1000 observed for the Si(113) facetting due to its larger average terrace width (400 Å).[16] Coincidentally, the areal rate of zippering found on Ni(977) closely resembles the rate observed on Si(113) in a higher temperature range, indicating some level of commonality in surface mass transport mechanisms across material types.

Summary

Using STM imaging at elevated temperature, we have observed the atomic-level details of step merging on Ni(977). Oxygen mediates a step-doubling transition on this stepped surface that occurs via zippering of adjacent steps. This result is consistent with extant theoretical models. Rates of step merging are fastest in the limit of step edge saturation of adsorbed oxygen. Merging responses of regions of various step densities to equivalent oxygen exposures indicate the existence of a critical concentration of oxygen as well as multiple pathways for oxygen motion and aggregation on the surface. As further evidence of the sensitivity of the step merging process to local oxygen coverage and local step configurations under conditions of high oxygen coverage, strong spatial and temporal correlations were found to exist between adjacent merging events. Here, merging motion was punctuated in time, presumably allowing adsorbate mobility and fluctuations to generate ideal local oxygen step decoration as well as necessary local step and kink geometries to facilitate doubling. The results of these experiments further confirm the delicacy of the equilibrium morphology for this stepped surface. By probing single events involved in the oxygen-driven morphological transformations of this stepped surface, we have expanded our understanding of the role of local structure in the initial steps of metallic

oxidation as well as the nature of surface transport mechanisms that lead to surface facetting.

Acknowledgment. The authors wish to thank Brent Mantooth for his assistance with figures and Seth Darling for many enlightening discussions. This research was supported by the Air Force Office of Scientific Research with further support from the NSF-Materials Research Science and Engineering Center at the University of Chicago, Grant DMR-9808595.

References and Notes

(1) Zambelli, T.; Wintterlin, J.; Trost, J.; Ertl, G. *Science* **1996**, *273*, 1688−1690.
(2) Kamna, M. M.; Stranick, S. J.; Weiss, P. S. *Science* **1996**, *274*, 118−119.
(3) Niu, L.; Gaspar, D. J.; Sibener, S. J. *Science* **1995**, *268*, 847−850.
(4) Schaak, A.; Nieuwenhuys, B.; Imbihl, R. *Surf. Sci.* **1999**, *441*, 33.
(5) Melechko, A. V.; Braun, J.; Weitering, H. H.; Plummer, E. W. *Phys. Rev. B* **2000**, *61*, 2235.
(6) Darling, S. B.; Hanbicki, A. T.; Pearl, T. P.; Sibener, S. J. *J. Phys. Chem. B* **1999**, *103*, 9805−9808.
(7) Hanbicki, A. T.; Darling, S. B.; Gaspar, D. J.; Sibener, S. J. *J. Chem. Phys.* **1999**, *111*, 9053−9057.
(8) Gaspar, D. J.; Hanbicki, A. T.; Sibener, S. J. *J. Chem. Phys.* **1998**, *109*, 1−9.
(9) Somorjai, G. A.; Hove, M. A. V. *Prog. Surf. Sci.* **1989**, *20*, 201.
(10) Williams, E. D.; Bartelt, N. C. *Science* **1991**, *251*, 393−400.
(11) Batteas, J. D.; Dunphy, J. C.; Somorjai, G. A.; Salmeron, M. *Phys. Rev. Lett.* **1996**, *77*, 534−537.
(12) Niu, L.; Koleske, D. D.; Gaspar, D. J.; King, S. F.; Sibener, S. J. *Surf. Sci.* **1996**, *356*, 144−160.
(13) Pearl, T. P.; Sibener, S. J. *J. Chem. Phys.*, in press.
(14) Pearl, T. P.; Sibener, S. J., submitted.
(15) Sudoh, K.; Yoshinobu, T.; Iwasaki, H.; Williams, E. D. *Phys. Rev. Lett.* **1998**, *80*, 5152.
(16) Sudoh, K.; Iwasaki, H.; Williams, E. D. *Surf. Sci.* **2000**, *452*, L287-L292.
(17) Song, S.; Yoon, M.; Mochrie, S. G. J.; Stephenson, G. B.; Milner, S. T. *Surf. Sci.* **1997**, *372*, 37.
(18) Khare, S. V.; Einstein, T. L.; Bartelt, N. C. *Surf. Sci.* **1995**, *339*, 353−362.
(19) Pearl, T. P.; Sibener, S. J. *Rev. Sci. Instrum.* **2000**, *71*, 124−127.
(20) Pearl, T. P.; Darling, S. B.; Sibener, S. J. *Surf. Sci.*, submitted for publication.
(21) Jeong, H.-C.; Williams, E. D. *Surf. Sci. Rep.* **1999**, *34*, 171−294.
(22) Vitos, L.; Skriver, H. L.; Kollár, J. *Surf. Sci.* **1999**, *425*, 212−223.